Cell Blebbing and Membrane Area Homeostasis in Spreading and Retracting Cells

Leann L. Norman,[†] Jan Brugés,[‡] Kheya Sengupta,[§] Pierre Sens,[‡] and Helim Aranda-Espinoza[†*]
[†]Fischell Department of Bioengineering, University of Maryland, College Park, Maryland; [‡]École Supérieure de Physique et de Chimie Industrielles de la Ville de Paris, Centre National de la Recherche Scientifique, UMR 7083, Paris, France; and [§]Centre National de la Recherche Scientifique, UPR 3118, Centre Interdisciplinaire de Nanosciences de Marseille, Aix-Marseille Université, Marseille, France

ABSTRACT Cells remodel their plasma membrane and cytoskeleton during numerous physiological processes, including spreading and motility. Morphological changes require the cell to adjust its membrane tension on different timescales. While it is known that endo- and exocytosis regulate the cell membrane area in a timescale of 1 h, faster processes, such as abrupt cell detachment, require faster regulation of the plasma membrane tension. In this article, we demonstrate that cell blebbing plays a critical role in the global mechanical homeostasis of the cell through regulation of membrane tension. Abrupt cell detachment leads to pronounced blebbing (which slow detachment does not), and blebbing decreases with time in a dynamin-dependent fashion. Cells only start spreading after a lag period whose duration depends on the cell's blebbing activity. Our model quantitatively reproduces the monotonic decay of the blebbing activity and accounts for the lag phase in the spreading of blebbing cells.

INTRODUCTION

Blebs are spherical outgrowths of the plasma membrane (PM) that occur upon membrane detachment from the underlying cytoskeleton. Traditionally viewed as a sign of apoptosis, blebs are increasingly emerging as dynamic features connected to dramatic cellular reorganization, with a role in both in vivo (1) and in vitro cell motility (2,3). Blebs have been observed during spreading (4–7), mitosis (6,8,9), and cell migration (10–12). The protrusion of cellular blebs has also been identified as a potential strategy for tumor cell migration (13,14). Various cell types including lymphocytes (15), *Dictyostelium* (12,13), and tumor melanoma cells (14) utilize bleb-mediated migration to navigate three-dimensional matrices, emphasizing the broad physiological importance of cellular blebbing. The mechanics of a single bleb is beginning to be well understood (16–18). Blebs are nucleated by the loss of PM-cytoskeleton adhesion, possibly due to the increase of cytoskeleton contractility (3,19). The freed membrane inflates rapidly (within 30 s) into a spherical bleb (5,6,16,18,20). Bleb expansion stalls either because of a drop of pressure inside the cell, or after de novo assembly of an actin cortical layer on the bleb membrane. First, trans-membrane actin-binding proteins localize within the membrane of the bleb, followed by polymerization of actin at the membrane of the bleb, and lastly, localization of motor proteins, in particular, myosin II (17). A new contractile cortex is formed, which retracts the bleb toward the cell body within a few minutes (6,16–18).

Cellular blebs can also be driven by external mechanical perturbations such as hyperosmotic shock or micropipette suction (21), or can result from the rupture of the cytoskeleton cortex (22). Blebs have also been identified as obligatory features after detachment of adhered cells (4–7,23). However, blebs have not yet been connected to the global mechanical homeostasis of the cell. We demonstrate this connection here by observing the blebbing activity of adherent cells abruptly detached from their substrate, and we further show the role blebs play in the initial stage of adhesion.

The dynamics of cell spreading has been studied for many individual cell types including fibroblasts (23,24) and neutrophils (25). Theoretical models of cell spreading have also been proposed (26,27), where spreading results from a balance between a driving force from substrate adhesion and/or actin polymerization, and a viscoelastic force accompanying cell deformation. Broadly speaking, such an approach predicts a power-law where the cell-substrate contact area increases linearly with time (the cell then essentially behaves as a very viscous fluid), up to a saturation area, that depends on both cell and substrate. Membrane tension could play an important role in opposing cell deformation, and the regulation of PM surface area by endosomal recycling through endo- and exocytosis mechanisms is thought to be required for major changes of the cell shape during cellular processes such as mitosis (9) and spreading (28–30). It has been shown that in addition to bringing specific adhesion proteins to the PM, increased exocytosis during cell spreading helps to prevent an increase of membrane tension by bringing membrane material to the PM (30,31), while endocytosis could play the opposite role during cell detachment (28,29). Mechanically speaking, it appears probable that membrane recycling is crucial in preventing a large variation of the PM tension during major morphological cell changes (9,30). We show below that blebs can also contribute to this mechanical homeostasis.

Submitted April 21, 2010, and accepted for publication July 16, 2010.

*Correspondence: helim@umd.edu

Editor: Levi A. Gheber.

0006-3495/10/09/1726/8 $2.00

doi: 10.1016/j.bpj.2010.07.031

MATERIALS AND METHODS

Cell culture and substrate preparation

Bovine aortic endothelial cells (BAECs) were purchased from Lonza Walkersville (Walkersville, MD) and cultured in Dulbecco Modified Eagle Medium supplemented with 10% bovine serum, 1% 200 mM L-glutamine, and 0.5% penicillin-streptomycin (referred to as BAEC medium). Cells were maintained at 5% CO_2, 70% humidity, and 37°C. Cells were passaged at 90% confluence, and used between passages 3 and 10 for experiments. Before each experiment, cells were starved of serum for ~16 h and detached with 0.25% trypsin with EDTA. Glass-bottom dishes (No. 1.5; MatTek, Ashland, MA) were coated with fibronectin (FN) by incubating with 100 μg/mL FN (Sigma-Aldrich, St. Louis, MO) at room temperature for 2 h. Dishes were rinsed three times with 1× phosphate-buffered saline before addition of cells.

Detachment experiments, spreading experiments, and actin staining

For detachment experiments, cells were plated on FN-coated plates for 24 h to reach saturation. For rapid detachment, cells were trypsinized with 0.25% trypsin with EDTA, while trypsin with EDTA diluted 20:1 with BAEC medium was used for slow detachment. For spreading experiments, cells were plated onto new BAEC media-filled FN-coated dishes after the appropriate incubation time (0–120 min). An average of 5×10^3 cells were plated per dish to ensure single cells during spreading. For detachment and spreading experiments, one frame was recorded every 3–5 s. To modify the number of blebbing cells without drug or osmotic treatment, cells were allowed to remain in suspension after trypsinization between 0 and 120 min before replating. Interference reflection microscopy (IRM) and bright-field (BF) snapshots were taken for a minimum of 15 random cells per spreading time point. To observe the number of blebs per cell, BAECs were plated onto extremely soft (E ~260 Pa), uncoated polyacrylamide gels (following previously described methods (32)). Individual cells were observed with multiple BF snapshots taken at each time point to ensure the identification of blebs on both the basal and apical surfaces. Cells were treated with 80 μM dynasore (Sigma-Aldrich) for 10 min before plating and remained in the same concentration of the drug for the entire duration of the experiment. Using all captured planes, the numbers of blebs were counted for each cell. Viability was verified for both dynasore-treated cells and control after 2 h of incubation. Furthermore, cells rinsed and removed from dynasore treatment were able to spread in a manner comparable to that of control cells. For actin staining, cells were fixed for 20 min with 2% paraformaldehyde solution, and permeabilized with 1% Triton-X for 5 min. A 2% bovine serum albumin solution was used to prevent nonspecific binding, and cells were stained with 0.1 M Phalloidin-TRITC.

Microscopy, imaging conditions, and data analysis

Interference reflection microscopy (IRM) is a method used to detect surface-to-surface distance. Typically, the areas of the membrane closest to the surface appear dark, while those further away look brighter; thus, IRM is well suited for cell adhesion studies. Spreading and detachment experiments were performed using IRM, while the number of blebs per cell was observed using bright-field microscopy. Cells were observed with an inverted microscope (Olympus America, Center Valley, PA) and fitted with a 100× oil immersion objective lens and a 100 W mercury lamp (Olympus). A charge-coupled device camera (Retiga SRV camera; QImaging, Surrey, British Columbia, Canada) was used for image recording. All experiments were performed in a closed microscope chamber (Precision Plastics, Beltsville, MD) to ensure characteristic culture conditions including 5% CO_2, 50% humidity, and 37°C.

The cell was identified using an algorithm based on fitting of intensity histograms which was implemented in IGOR-Pro data analysis software (WaveMatrix, Portland, OR). For a detailed explanation of this method and the algorithms used to fit intensity histograms, refer to Sengupta et al. (25). For statistical evaluations of spreading areas, IRM images were analyzed using ImageJ (National Institutes of Health, Bethesda, MD) software. The cell-boundaries were traced by hand and area was calculated using built-in ImageJ routines.

RESULTS AND DISCUSSION

Blebs appear after rapid cell detachment

We observed blebbing activity of adherent cells by imaging the cell region near the substrate using IRM. Fig. 1 *A* shows blebs in adhering bovine aortic endothelial cells (BAEC), which appeared as spherical protrusions in BF and fluorescence microscopy and corresponded to uniformly dark circular adhesion zones when attached to the substrate, using IRM. Blebs had a similar morphology to those observed in fibroblasts (4,8) and human melanoma cells (6,17,18), and their extension and retraction rates were also similar to those previously reported (17).

Rapid cell detachment with trypsin (as well as detachment with EDTA) led to the appearance of numerous blebs. A typical process of moderately rapid cell detachment is shown in Fig. 1 *B* using IRM. In this particular case, blebs

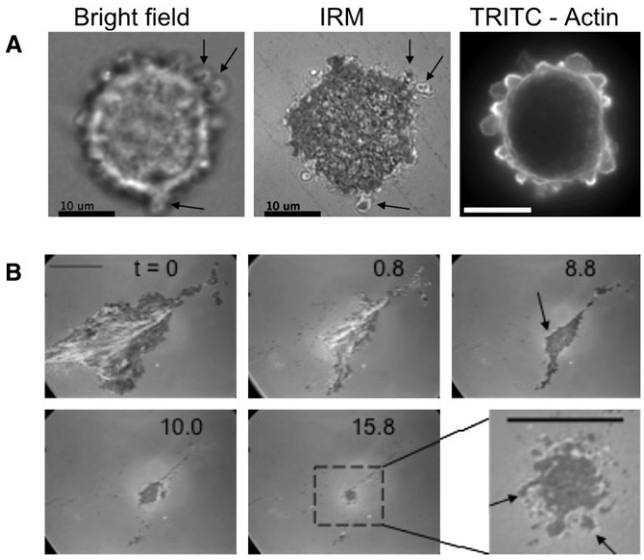

FIGURE 1 (*A*) Identification of cellular blebs during detachment and spreading using interference reflection microscopy (IRM). Bovine aortic endothelial cells (BAEC) were observed using bright-field (BF) and phalloidin-TRITC staining, and showed characteristic adhesion patterns when using IRM (*arrows*). IRM and BF images were captured within 10 s for the same cell, while actin staining was performed on fixed cells. Scale bar is 10 μm. (*B*) Using IRM, blebs were observed on the basal surface during trypsin detachment (t = min after addition of trypsin). Blebbing was first noted on only a small area of the cell at $t = 8.8$ (*arrow*), and became more numerous and larger after 10 min (Scale bar is 25 μm). $t = 15.8$ is enlarged (scale bar is 10 μm) to illustrate some of the blebs (*arrows*).

were first observed after 8.8 min (Fig. 1 *B*), and became more numerous and larger after 10 min. In our hands, the time of bleb appearance was arbitrary; however, the detachment area necessary for bleb appearance was consistent for cells of similar initial adhesion areas. Typically, blebs began to appear on both the basal and apical surface of detaching cells ($N = 6$) after ~78 $\pm$ 11% of the total adhered area was detached.

The appearance of blebs during detachment could be due to major disruption of the cytoskeleton structure. It could also be a way for the cell to deal with the large amount of membrane area that was transferred to the PM during cell spreading, and that will eventually be endocytosed (28,29). We tested the role of the kinetics of cell detachment by using a lower concentration of trypsin. Interestingly, blebbing was not observed when cells were detached over more extended periods of time (>50 min in our case; see Movie S1 and Movie S2 in the Supporting Material). The timescale involved appears fairly large as compared to cytoskeleton remodeling times, but is rather consistent with the dynamics of membrane recycling (33,34). Although trypsin cleaves cell surface receptors during detachment, it has been illustrated that this does not significantly affect the readhesion or spreading saturation of cells (35). In fact, when DNA and RNA synthesis are inhibited before and after trypsinization, there remains no effect on the ability of cells to readhere and spread (35), emphasizing that readhesion is not dependent on the resynthesis or expression of new cell-surface receptors after detachment. Effects in readhesion after trypsinization are reported only when temperature is dramatically reduced compared to physiological norms (35,36). To gain more insight on the relation between blebbing and membrane recycling, we studied the evolution of the blebbing activity of cells after fast detachment.

Endocytosis regulates cell blebbing

Adhered BAEC were rapidly detached using a high concentration of trypsin, and then placed on soft polyacrylamide gels (E ~260 Pa), without extracellular matrix coating, making the substrate nonadherent. The number of blebs was counted using BF microscopy to monitor the evolution with time of the number of blebs per cell (Fig. 2). For control cells, the average number of blebs remained fairly constant for the first 10–15 min. After 15 min, we observed a gradual decrease in the number of blebs per cell until 40–60 min, when blebbing ceased. The large characteristic timescale of the blebs disappearance suggests that the number of blebs is likely to be regulated by membrane internalization mechanisms such as endocytosis (28,29).

To test this hypothesis, we repeated the above experiment with cells treated (after detachment) with 80 μM dynasore, an inhibitor of dynamin-dependent endocytotic pathways (37). Although the number of blebs did decrease slightly over the observed 90-min period, the majority of cells

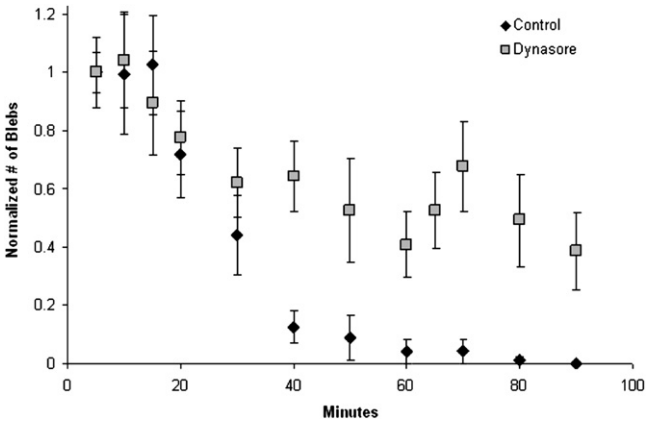

FIGURE 2 The number of blebs per cell decreased with time spent in suspension. BAEC were plated onto extremely soft, uncoated polyacrylamide gels which prevented cell attachment and spreading. Cells were observed with multiple BF snapshots taken at each time point to ensure the identification of blebs on both the basal and apical surfaces. The normalized number of blebs per cell (compared to the number of blebs 5 min after detachment) is plotted with error bars representing standard error. Control cells (N = 10–20) maintained a constant number of blebs for the first 15 min, and then exhibited a continuous decrease in blebbing over time, with all blebs disappearing after 90 min. For dynasore-treated cells (N = 10) there is a slight decrease in blebbing over time; however, only one of the 10 observed cells ceased blebbing after 90 min.

treated with dynasore were unable to completely reintegrate cellular blebs (Fig. 2). Furthermore, cells treated with dynasore did not spread on uncoated polyacrylamide gels or fibronectin-coated glass substrates. We observed cells for up to 3.5 h during which the adhered area did not increase, although the majority of cells continued to bleb.

Role of blebs in cell spreading

Finally, we established the influence of blebs on the kinetics of cell spreading. Adherent cells rapidly detached by trypsinization were replated after varying times of incubation (0–120 min), and their spreading area was captured by IRM (Fig. 3 *A*). Cells plated immediately after trypsinization typically exhibited vigorous blebbing (Fig. 3 *A* and Movie S3), while cells which remained in solution for 120 min before plating did not bleb (Fig. 3 *A*, nonblebbing cell and Movie S4).

Nonblebbing cells displayed both filopodia and lamella (respectively, *white* and *black arrowheads* in Fig. 3 *A*, and see Movie S4), within the first 10 min of spreading. They spread quickly on the substrate, following the linear dynamics reported previously (26). On the contrary, the initial substrate adhesion of blebbing cells occurred through individual bleb-adhesion zones (Fig. 3 *A*, *arrow*), which grew and fused to form the adhered area of the cell. Because of constant bleb retraction, this process was very slow, and little increase of the adhered area was actually observed during the first 40 min. During this long lag spreading

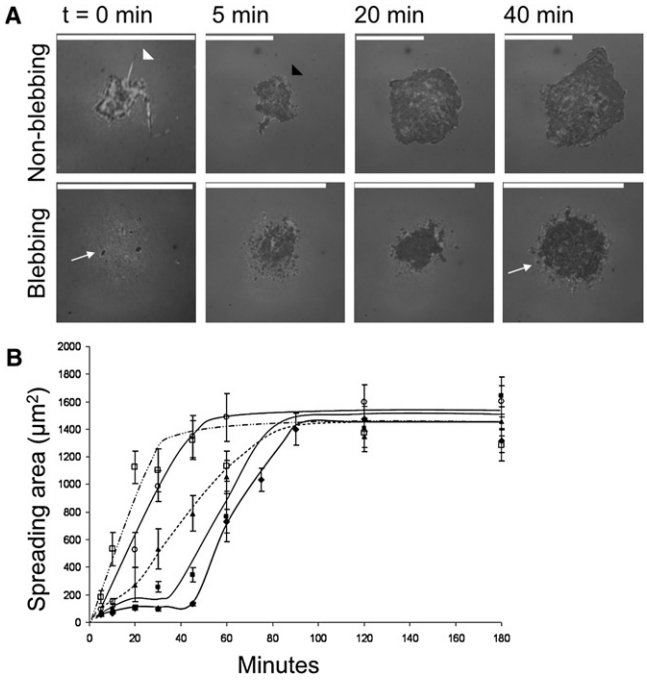

FIGURE 3 (*A*) Differences in initial spreading behavior were observed for individual blebbing and nonblebbing cell spreading events. For nonblebbing cells, features of fast growth including filopodia (*white arrowhead*) and lamella (*black arrowheads*) were present within the first 10 min of spreading. Blebbing cells attached initially to the substrate through individual bleb adhesions (*white arrow*, $t = 0$ min) and continued to bleb for up to 40 min. After 40 min, fast cell spreading occurred with a similar speed to that of nonblebbing cells. (Scale bar is 25 μm.) (*B*) Effect of time for which cells were suspended in solution before plating on cell spreading behavior. Suspension time = 0 (◆), 15 (■), 30 (▲), 60 (○), or 120 (□) min before plating. BF and IRM for a minimum of 15 random cells were captured for each time point. Error bars display standard error, with lines serving as guides to the eye.

regime, the cell showed numerous blebs at the periphery of the adhesion zone, which dynamically adhered and detached from the substrate. Lamella and filopodia became apparent after some time and initiated the fast spreading regime; after that, blebs quickly disappeared from the PM. The timescale for bleb disappearance was similar for spreading and nonspreading cells (Fig. 2), illustrating that the reintegration of cellular blebs is independent of cell spreading, and is more likely regulated by internalization mechanisms such as endocytosis (28,29). Furthermore, the spreading rate in the fast spreading regime was similar for blebbing and nonblebbing cells (33 ± 17 μm^2/min, $N = 9$ and 30 ± 18 μm^2/min, $N = 9$, respectively), emphasizing that the major difference between the two spreading behaviors lies in the first 40 min of spreading—the time needed for blebs to disappear.

To support this claim, we incubated cells for varying time before replating them and then measured the area from IRM snapshots for a minimum of 15 random cells taken at each time point during spreading (Fig. 3 *B*). A lag was still observed for cells incubated <60 min, but the extent of the lag phase decreased with increasing incubation time, consistent with the view that the lag phase is connected with the presence of blebs. Cells incubated for 60 min or more quickly developed lamella and spread very fast. Here again, the fast spreading regime was similar for all cases, whether it was preceded by a lag phase or not, as was also the final adhered area at saturation. We examined the number of cells that were blebbing during the spreading process and found that the percentage of cells blebbing decreased with incubation time, with 92% of the $t = 0$ min incubation cells blebbing, while only 62% and 33% of cells are blebbing after 30 and 60 min, respectively. Cells no longer bleb after 120 min of incubation. Replating of EDTA-detached cells produced similar incubation-dependent dynamics comparable to those shown in Fig. 3 *B* (data not shown).

Model

The aim of the theoretical model is to obtain a general description for the kinetics of cell adhesion that includes area recycling between the plasma membrane (PM) and area storage within membrane blebs. The model presented below uses a general linear viscoelastic framework to relate cell deformation to membrane tension, and is not restricted to cell spreading. It seeks to reproduce the kinetic evolution of parameters that can be directly observed in the experiments, namely the cell area in contact with the substrate (which we call A_c) and the number of blebs in the cell N_b. All other variables introduced in the model, and in particular the various relevant tensions, are relative variables which are chosen to vanish in the reference state of a fully relaxed, nonadhering cell. Blebs influence the membrane tension by sequestering membrane area, and are taken into account by introducing formation and retraction rates that depend on membrane tension.

Viscoelastic description of cell spreading

From a mechanical point of view, a cell is a very complex viscoelastic system powered by energy consumption. Nevertheless, it has been theoretically proposed and experimentally verified (26,27) that as far as spreading is concerned, the cell essentially behaves as a viscous drop. The adhered area kinetics follows from a balance of forces between the adhesion driving force (characterized by an adhesion energy per unit area ϵ) and a viscous dissipation,

$$\eta_c \dot{A}_c = \epsilon,$$

where η_c (energy $\times$ time/length^4) characterizes energy dissipation during cell spreading and is mostly controlled by viscous flow through the cytoskeleton cortex as the cell spreads (26). Cells stop spreading after a while, meaning that some elastic stress must be stored during spreading, which eventually balances the adhesive driving force at large strain. Here, we assume that this elastic stress is stored

as membrane tension γ_m, and replace the spreading equation above by

$$\eta_c \dot{A}_c = \epsilon - \gamma_m.$$

Membrane tension is the only force opposing deformation (see below), leading to a saturation when it balances the driving force: $\gamma_m = \epsilon$. By analogy with giant unilamellar vesicles (38), in which the membrane tension is known to be related to the difference between the apparent area and the true membrane area (called A_m), we adopt the simple linear relationship

$$\gamma_m = k_m(A_c - A_m),$$

where k_m is the membrane effective stretching modulus. Note that this relationship should be understood in a phenomenological way, where the adhered area A_c is used as a measure of the cell deformation (it vanishes for an undeformed cell in solution). The stretching modulus k_m is thus a phenomenological parameter, which need not be equal (although it should be of the same order of magnitude) to the cell stiffness measured under different kinds of deformation.

The plasma membrane of a cell constantly exchanges material with the cell interior by endo- and exocytosis, with the entirety of the PM being recycled over ~1 h (33). The rate of endocytosis is known to inversely correlate with the tension of the plasma membrane (39), and a general relationship between rates of membrane transport and difference of membrane tensions within the cell can be expected (40,41). To translate these facts into a mechanical equation, we assume that the balance of endo- and exocytosis depends on the difference between the membrane tension and the tension γ_i of inner organelles (e.g., the Golgi), again assuming linear kinetics for the total area of the cell surface $\mathcal{A}'_m = A_m + A_b$, which includes the PM area, and also the area A_b contained in blebs:

$$\eta_i \dot{\mathcal{A}}'_m = \gamma_m - \gamma_i.$$

Finally, to comply with our assumption that cell spreading is eventually limited by an increase of membrane tension, the inner tension is assumed to increase as area is transferred to the PM:

$$\gamma_i = k_i \mathcal{A}'_m.$$

Combining all the rules described above, and defining the effective parameters

$$k_1 = k_m^2/(k_m + k_i), k_2 = k_m k_i/(k_m + k_i), \text{and}$$
$$\tau_m = \eta_i/(k_m + k_i),$$

the evolution of the adhered area is described by

$$\eta_c \dot{A}_c = \epsilon - \gamma_m$$
$$\text{with} \qquad (1)$$
$$\dot{\gamma}_m + \frac{\gamma_m}{\tau_m} = (k_1 + k_2)\dot{\mathcal{A}}_m + \frac{k_2}{\tau_m}\mathcal{A}_m,$$

where $\mathcal{A}_m = A_c + A_b$ is the apparent PM area and includes the area sequestered in blebs. We will see below that the bleb area A_b is fixed by the membrane tension γ_m, so this set of equations uniquely determines both the cell shape and its mechanical properties (A_c and γ_m, respectively). The dynamical model sketched in Fig. 4 *A* and leading to Eq. 1 for the tension γ_m is equivalent to a viscoelastic model depicted in Fig. 4 *B*, consisting of the so-called standard linear elastic model (a Maxwell fluid of stiffness k_1 and relaxation time τ_m, in parallel with a spring of stiffness k_2) for the total PM area $\mathcal{A}_m$. In the absence of blebs, the membrane crosses-over from a relatively stiff elastic body at short time to a much softer elastic body after a relaxation time τ_m, identified with the characteristic time of membrane area homeostasis (of ~40 min for BAEC). As we show

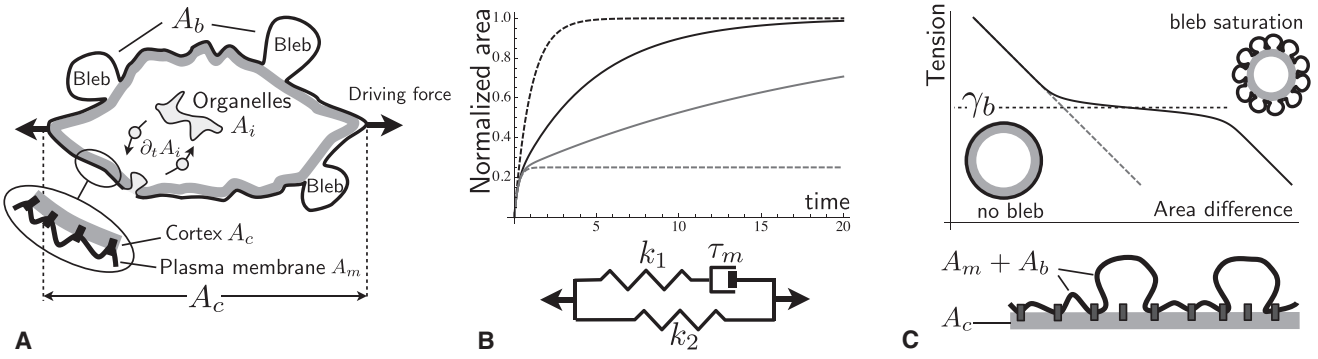

FIGURE 4 Viscoelastic model for cell deformation. (*A*) Sketch of the cellular model: upon a perturbation that modifies the shape of the cell (area A_c), membrane recycling with internal organelles (timescale τ_m), and blebbing (bleb area A_b) regulate membrane tension and cell deformation. (*B*) Equivalent viscoelastic cellular model applying to the area $A_c + A_b$. (*Spring* and *dashpot*) Linear elastic and viscous components, respectively, indicating kinetics of cell spreading under a constant driving force (the time is normalized by the typical spreading time $\tau_c = \eta_c/k_2$). (*Dashed* and *solid curves*) Purely elastic cells with very fast and very slow area transfer ($\tau_m \to 0$ and $\tau_m \to \infty$, respectively). (*Shaded* and *solid curves*) Membrane area transfer $\tau_m = 10\tau_c$ and $\tau_m = 2\tau_c$, respectively, with $k_1 = 3.4k_2$. (*C*) Relationship between the membrane tension and the cortex to plasma membrane area difference ($A_m + A_b - A_c$). (*Dashed lines*) Absence of blebs; (*solid lines*) with blebs. The latter shows that blebs maintain the membrane tension to a characteristic value γ_b, upon increase of the area difference.

below, blebs appear if the membrane tension drops below a critical value (Fig. 4 *C*).

Bleb statistics

The life cycle of a bleb involves nucleation and growth, followed by the polymerization of a new actin cortex underneath the bleb membrane and by bleb retraction. The whole process only takes a few minutes, and in the timescale of our observations (~1 h), it can be considered instantaneous. The average number of blebs per cell thus results from a balance between nucleation and retraction. The rate of bleb retraction depends mostly on the time needed to polymerize an actin cortex and recruit myosin, and can be considered roughly constant. The rate of bleb nucleation, on the other hand, strongly depends on membrane tension.

It has been shown that the energetics of bleb formation is mostly controlled by three physical parameters: internal cell pressure, the membrane-cortex adhesion energy, and the membrane tension (see (16) and the Supporting Material). While the internal cell pressure, partly built by acto-myosin contraction, promotes membrane cortex separation and membrane inflation, the other two physical parameters oppose bleb formation. As a result, the bleb energy displays the characteristic features of a nucleation process: if the membrane area detached from the cortex is small, it rebinds without major inflation; but beyond a critical area, corresponding to a particular nucleation energy, blebs steadily inflate. The smaller the nucleation energy barrier, the higher the probability to observe blebs on a given cell. It has been suggested that local increases of the cortical activity could be responsible for bleb nucleation (16,18). Because the nucleation energy depends on the membrane tension (linearly, see the Supporting Material), blebbing can also be triggered by a major drop in membrane tension, such as the one expected upon detachment of a strongly adhered cell.

The rate of bleb nucleation is expected to grow exponentially with the nucleation energy barrier, hence with membrane tension. The fraction of the cell surface covered with blebs thus takes the general form (see the Supporting Material)

$$n_b = \frac{1}{1 + e^{\beta(\gamma_m - \gamma_b)}}, \qquad (2)$$

where γ_b and β are, respectively, the threshold tension for blebbing and the bleb nucleation sensitivity to membrane tension. They are expressed in terms of physical parameters in the Supporting Material. Equation 2 tells us that there should be no blebs for high membrane tensions, while blebs should saturate the cell surface ($n_b \sim 1$) for low tensions, with a transition at $\sim\gamma_b$, the sharpness of which is controlled by β. Bleb formation is physically very similar, although for different energy and length scales, to the invagination of protein-enriched membrane domains such as caveolae (42), which have been shown to buffer membrane tension. The total area in blebs is the bleb fraction times the maximal area that can be contained in blebs: $A_b = A_{b0} n_b$.

Model predictions

Solving Eq. 1 in the absence of blebs can be done analytically (see the Supporting Material), and examples of such spreading curves are presented in Fig. 4 *B*. Initial spreading is linear with time with a rate ϵ/η_c (of ~0.5 $\mu m^2/s$, Fig. 3), and the subsequent spreading kinetics depend on the recycling time τ_m. If membrane recycling is fast, $\tau_m << \tau_c$ with $\tau_c = \eta_c/k_2$, the cell behaves as a soft body of stiffness k_2 and spreading saturates after a time τ_c to an area ϵ/k_2. In the absence of recycling, on the other hand, the spreading saturates to a much smaller area $\epsilon/(k_1 + k_2)$. In the physiologically relevant limit $\tau_m > \tau_c$, the initial spreading kinetics are controlled by viscous dissipation in the cytosol, but the later stage is slower and controlled by the kinetics of area transfer.

A large fraction of internal area is transferred to the PM during cell spreading. Upon rapid cell detachment, most of the cell's adhered area retracts very quickly (see Fig. 1), without rapid change of the PM area. The excess area gained upon spreading results in a large drop of membrane tension (see the Supporting Material). If the tension drops below γ_b (Eq. 2), blebs form on the cell surface and take up part of the excess area, thereby buffering the tension to a value close to γ_b. Mechanically, blebs thus behave in a way reminiscent of smaller membrane outgrowth such as caveolae (42), which can regulate membrane tension by sequestering excess membrane area. The membrane tension may, however, drop further if the excess membrane area becomes so large that the cell surface is saturated by blebs ($n_b \simeq 1$). After a time of $\sim\tau_m$, endocytosis slowly recycles the PM excess area, also removing bleb membrane area, until the rest tension is reached. The number of blebs on the PM decays in time with a characteristic timescale τ_m. We present the numerical solution of Eqs. 1 and 2 for the decay of the number of blebs on the PM with time in Fig. 5 *A*, where parameters have been chosen to reproduce our experimental observation (Fig. 2). The number of blebs remains constant for some time before decreasing because the cell was initially saturated with blebs ($n_b \simeq 1$). This can be expected in the case of strong adhesion, where the large membrane area transferred to the PM during spreading causes a massive drop of tension upon detachment. In the opposite limit of weak adhesion ($\epsilon < -k_2/k_1\gamma_b$, only relevant if $\gamma_b < 0$, see the Supporting Material), even rapid cell detachment will not result in cell blebbing.

The full system of kinetic equations used to determine the kinetics of cell spreading and retraction is given in the Supporting Material. We calculated the adhesion kinetics after different incubation times by choosing as initial conditions different points along the relaxation curve $n_b(t)$ (*squares*, Fig. 5 *A*). The observed adhesion kinetics (Fig. 3) could be reproduced (Fig. 5 *B*) by assuming that

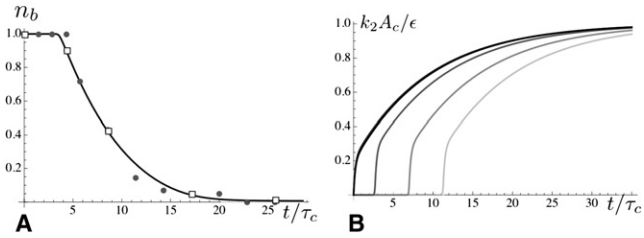

FIGURE 5 (*A*) Evolution of the (normalized) average number of blebs per cell n_b with time. In both the experimental observations (*shaded points*, from Fig. 2) and the theoretical curve, cells were allowed to spread until complete saturation before being detached from the substrate, leading to pronounced blebbing. Theoretically, n_b was quantified using Eqs. 1 and 2 by fixing $\epsilon = 0$ and $A_c = 0$ (no spreading) and setting the initial membrane area to its value for a fully adhered cell: $\mathcal{A}_m = \epsilon/(k_2(1 + k_2/k_1))$. Parameters are the same as in Fig. 4, with $\epsilon/k_2 = 1500\ \mu m^2$ (during the spreading phase), $\tau_c = 3.5$ min, $\gamma_b = -0.1\epsilon$, $\beta\epsilon = 50$, and $A_{b0} = \epsilon/(4k_2)$. (*B*) Spreading kinetics for different incubation times (*squares* in panel *A*), increasing from zero (*lighter shading*) to infinity (*solid*), with $n_b{}^* = 0.25$.

the presence of blebs reduces the energy of adhesion between the cell and the substrate, which we render using the effective adhesion energy

$$\tilde{\epsilon} = \left(1 - n_b/n_b^*\right)\epsilon$$

(see the Supporting Material). We find that blebs prevented adhesion ($\tilde{\epsilon} \leq 0$) when blebs covered $> n_b{}^* = 25\%$ of the PM surface. This effect can be traced to the fact that the blebs do not seem to promote strong substrate adhesion, and to the repulsive pressure exerted by inflating blebs colliding with the substrate. Finally, we remark that the maximal area at saturation ($\sim\epsilon/k_2$) is independent of whether the cells were initially blebbing.

Our model predicts saturation of spreading when the adhesion energy is balanced by membrane tension, corresponding to a well-defined spreading area. It has been recently reported (30) that the force needed to extract a membrane tether from a spreading cell (which is related to the PM tension), does not increase, but instead, decreases during spreading. The authors concluded (as we do here) that tension is regulated via membrane recycling. However, their observation is inconsistent with our assumption that membrane tension is responsible for the saturation of cell spreading. Tether force is not only influenced by membrane tension, but also by membrane cytoskeleton interaction, and alteration of the latter could be responsible for the observations of Gauthier et al. (30). However, if membrane tension indeed decreases during spreading, another global cellular phenomenon must limit spreading. This detail could invalidate our prediction concerning saturation (although our main prediction, that the saturated area does not depend upon blebbing, is validated by our observations), but would not change our picture of 1), the way blebbing is related to membrane homeostasis, and 2), the effects blebs have on the initial cell spreading pattern.

CONCLUSIONS

Along with cytoskeleton remodeling, major cellular shape changes such as those occurring during mitosis, apoptosis, and cell motility are regulated by membrane recycling (9,43). In addition to bringing specific proteins to the PM, membrane recycling also permits membrane area homeostasis, which insures that the right amount of membrane area is available for a particular transformation (41). In the absence of such regulation, large deformation would be prevented by an excessive membrane tension. Membrane recycling is typically fairly slow (~30 min (33)), and the cell has other means to respond to sudden changes of PM tension, e.g., through membrane invaginations such as caveolae (42). Here we propose that cellular blebs can transiently play a similar role.

Our model could reproduce the slow disappearance of blebs by assuming a linear relationship between the flux of membrane and the difference of tension between the PM and internal organelles (41), extracting a typical membrane recycling time $\tau_m = 7$ min (Fig. 5). Remarkably, slowing cell detachment down did not lead to blebbing. This illustrates a property shared by all viscoelastic bodies, namely, that the strength of the response depends on the rate of the perturbation compared to the rate of internal relaxation. If cell detachment occurs sufficiently slowly for membrane homeostasis to regulate PM area, the PM tension is kept constant and blebs do not form.

While nonblebbing cells spread quickly as previously described (26), blebbing cells exhibited a lag phase during which blebs were seen to collide with and retract from the substrate, with little expansion of the adhered area (see Movie S3). We showed (Fig. 5) that this observation could be explained if blebs act as a pressurized cushion preventing cytoskeleton-mediated adhesion to the substrate. Indeed, the termination of the lag phase and the initiation of the fast spreading regime coincided with the disappearance of blebs. Cells replated immediately upon detachment, showed a long lag phase consistent with the bleb decay time of cells in suspension (Fig. 3 *B*), and the duration of the lag phase decreased with increasing incubation time. Interestingly, both blebbing and nonblebbing cells spread at similar pace during their fast spreading regime, and reached similar spreading areas at saturation. Therefore, although blebs can serve as a reservoir of area (7,17), blebs inhibit initial cell spreading because of direct interaction with the substrate but do not influence the final state. To emphasize that the bleb-related dynamics we observe in Fig. 3 is not dependent on the substrate coating, we plated blebbing cells onto polylysine-coated glass-bottom dishes and report no statistical differences between spreading behaviors during the first 4 h of spreading compared to fibronectin-coated dishes (data not shown).

In conclusion, this work illustrates that blebs are more than just an interesting cellular protrusion or a marker of cell apoptosis. Rather, cellular blebs are complex dynamic

structures that prevent initial cell spreading and play a critical role in the global mechanical homeostasis of the cell through regulation of membrane tension. The role of cellular blebs in maintaining cellular homeostasis may also have potential implications in bleb-based motility observed in vivo (1).

SUPPORTING MATERIAL

One figure, six equations, and four movies are available at http://www.biophysj.org/biophysj/supplemental/S0006-3495(10)00903-3.

H.A.-E. was supported by the Maryland Higher Education Commission under National Science Foundation grant No. CMMI-0643783, and L.L.N. was supported by a U.S. Army CREST fellowship. J.B. and P.S. acknowledge support from the French Agence Nationale pour la Recherche.

REFERENCES

1. Blaser, H., M. Reichman-Fried, …, E. Raz. 2006. Migration of zebrafish primordial germ cells: a role for myosin contraction and cytoplasmic flow. *Dev. Cell.* 11:613–627.
2. Charras, G., and E. Paluch. 2008. Blebs lead the way: how to migrate without lamellipodia. *Nat. Rev. Mol. Cell Biol.* 9:730–736.
3. Paluch, E., C. Sykes, …, M. Bornens. 2006. Dynamic modes of the cortical actomyosin gel during cell locomotion and division. *Trends Cell Biol.* 16:5–10.
4. Höglund, A. S. 1985. The arrangement of microfilaments and microtubules in the periphery of spreading fibroblasts and glial cells. *Tissue Cell.* 17:649–666.
5. Bereiter-Hahn, J., M. Lück, …, M. Vöth. 1990. Spreading of trypsinized cells: cytoskeletal dynamics and energy requirements. *J. Cell Sci.* 96:171–188.
6. Cunningham, C. C. 1995. Actin polymerization and intracellular solvent flow in cell surface blebbing. *J. Cell Biol.* 129:1589–1599.
7. Erickson, C. A., and J. P. Trinkaus. 1976. Microvilli and blebs as sources of reserve surface membrane during cell spreading. *Exp. Cell Res.* 99:375–384.
8. Laster, S. M., and J. M. Mackenzie, Jr. 1996. Bleb formation and F-actin distribution during mitosis and tumor necrosis factor-induced apoptosis. *Microsc. Res. Tech.* 34:272–280.
9. Boucrot, E., and T. Kirchhausen. 2007. Endosomal recycling controls plasma membrane area during mitosis. *Proc. Natl. Acad. Sci. USA.* 104:7939–7944.
10. Zhao, M., B. Song, …, J. M. Penninger. 2006. Electrical signals control wound healing through phosphatidylinositol-3-OH kinase-γ and PTEN. *Nature.* 442:457–460.
11. Langridge, P. D., and R. R. Kay. 2006. Blebbing of *Dictyostelium* cells in response to chemoattractant. *Exp. Cell Res.* 312:2009–2017.
12. Yoshida, K., and T. Soldati. 2006. Dissection of amoeboid movement into two mechanically distinct modes. *J. Cell Sci.* 119:3833–3844.
13. Lämmermann, T., and M. Sixt. 2009. Mechanical modes of 'amoeboid' cell migration. *Curr. Opin. Cell Biol.* 21:636–644.
14. Sahai, E., and C. J. Marshall. 2003. Differing modes of tumor cell invasion have distinct requirements for Rho/ROCK signaling and extracellular proteolysis. *Nat. Cell Biol.* 5:711–719.
15. Haston, W. S., and J. M. Shields. 1984. Contraction waves in lymphocyte locomotion. *J. Cell Sci.* 68:227–241.
16. Charras, G. T., M. Coughlin, …, L. Mahadevan. 2008. Life and times of a cellular bleb. *Biophys. J.* 94:1836–1853.
17. Charras, G. T., C. K. Hu, …, T. J. Mitchison. 2006. Reassembly of contractile actin cortex in cell blebs. *J. Cell Biol.* 175:477–490.
18. Charras, G. T., J. C. Yarrow, …, T. J. Mitchison. 2005. Non-equilibration of hydrostatic pressure in blebbing cells. *Nature.* 435:365–369.
19. Paluch, E., J. van der Gucht, and C. Sykes. 2006. Cracking up: symmetry breaking in cellular systems. *J. Cell Biol.* 175:687–692.
20. Dai, J., and M. P. Sheetz. 1999. Membrane tether formation from blebbing cells. *Biophys. J.* 77:3363–3370.
21. Merkel, R., R. Simson, …, E. Sackmann. 2000. A micromechanic study of cell polarity and plasma membrane cell body coupling in *Dictyostelium*. *Biophys. J.* 79:707–719.
22. Paluch, E., …, M. Piel, …, C. Sykes. 2005. Cortical actomyosin breakage triggers shape oscillations in cells and cell fragments. *Biophys. J.* 89:724–733.
23. Dubin-Thaler, B. J., J. M. Hofman, …, M. P. Sheetz. 2008. Quantification of cell edge velocities and traction forces reveals distinct motility modules during cell spreading. *PLoS ONE.* 3:e3735.
24. Döbereiner, H. G., B. Dubin-Thaler, …, M. P. Sheetz. 2004. Dynamic phase transitions in cell spreading. *Phys. Rev. Lett.* 93:108105-1–108105-4.
25. Sengupta, K., H. Aranda-Espinoza, …, D. Hammer. 2006. Spreading of neutrophils: from activation to migration. *Biophys. J.* 91:4638–4648.
26. Cuvelier, D., M. Théry, …, L. Mahadevan. 2007. The universal dynamics of cell spreading. *Curr. Biol.* 17:694–699.
27. Chamaraux, F., S. Fache, …, B. Fourcade. 2005. Kinetics of cell spreading. *Phys. Rev. Lett.* 94:158102–158104.
28. del Pozo, M. A., N. B. Alderson, …, M. A. Schwartz. 2004. Integrins regulate Rac targeting by internalization of membrane domains. *Science.* 303:839–842.
29. del Pozo, M. A., N. Balasubramanian, …, M. A. Schwartz. 2005. Phospho-caveolin-1 mediates integrin-regulated membrane domain internalization. *Nat. Cell Biol.* 7:901–908.
30. Gauthier, N. C., O. M. Rossier, …, M. P. Sheetz. 2009. Plasma membrane area increases with spread area by exocytosis of a GPI-anchored protein compartment. *Mol. Biol. Cell.* 20:3261–3272.
31. Balasubramanian, N., D. W. Scott, …, M. A. Schwartz. 2007. Arf6 and microtubules in adhesion-dependent trafficking of lipid rafts. *Nat. Cell Biol.* 9:1381–1391.
32. Norman, L. L., R. J. Oetama, …, H. Aranda-Espinoza. Modification of cellular cholesterol content affects traction force, adhesion and cell spreading. *Cell Mol. Biol.* 3:151–162.
33. Steinman, R. M., I. S. Mellman, …, Z. A. Cohn. 1983. Endocytosis and the recycling of plasma membrane. *J. Cell Biol.* 96:1–27.
34. Grant, B. D., and J. G. Donaldson. 2009. Pathways and mechanisms of endocytic recycling. *Nat. Rev. Mol. Cell Biol.* 10:597–608.
35. Kolodny, G. M. 1972. Effect of various inhibitors of readhesion of trypsinized cells in culture. *Exp. Cell Res.* 70:196–202.
36. Deman, J. J., and E. A. Bruyneel. 1977. Thermal transitions in the adhesiveness of HeLa cells: effects of cell growth, trypsin treatment and calcium. *J. Cell Sci.* 27:167–181.
37. Macia, E., M. Ehrlich, …, T. Kirchhausen. 2006. Dynasore, a cell-permeable inhibitor of dynamin. *Dev. Cell.* 10:839–850.
38. Evans, E., and W. Rawicz. 1990. Entropy-driven tension and bending elasticity in condensed-fluid membranes. *Phys. Rev. Lett.* 64:2094–2097.
39. Raucher, D., and M. P. Sheetz. 1999. Membrane expansion increases endocytosis rate during mitosis. *J. Cell Biol.* 144:497–506.
40. Upadhyaya, A., and M. P. Sheetz. 2004. Tension in tubulovesicular networks of Golgi and endoplasmic reticulum membranes. *Biophys. J.* 86:2923–2928.
41. Morris, C. E., and U. Homann. 2001. Cell surface area regulation and membrane tension. *J. Membr. Biol.* 179:79–102.
42. Sens, P., and M. S. Turner. 2006. Budded membrane microdomains as tension regulators. *Phys. Rev. E Stat. Nonlin. Soft Matter Phys.* 73:031918.
43. Kupfer, A., P. J. Kronebusch, …, S. J. Singer. 1987. A critical role for the polarization of membrane recycling in cell motility. *Cell Motil. Cytoskeleton.* 8:182–189.